A Dynamic Damage Model for the Rock-Shed Roof Under the Rockfall

hongyan liu (lhy1204@cugb.edu.cn)
China University of Geosciences (Beijing)

Research Article

Keywords: rockfall, impact force, the rock-shed roof, a dynamic damage model, Hertz contact theory

Posted Date: May 20th, 2021

DOI: https://doi.org/10.21203/rs.3.rs-478396/v1

A dynamic damage model for the rock-shed roof under the rockfall

Hongyan Liu [a,b*]

[a] College of Engineering & Technology, China University of Geosciences (Beijing), Beijing 100083, China

[b] Key Laboratory of Deep Geodrilling Technology of Ministry of Natural Resources, Beijing 100083, China

*corresponding author: lhy1204@cugb.edu.cn. ORCID: 0000-0001-7163-0702.

Abstract: The dynamic response of the rock-shed roof under the rockfall is a complicated mechanical process, which mainly includes the following three deformation stages, e.g. the elastic compression, plastic damage compression and elastic resilience stages of the rock-shed roof. However, the existing models based on Hertz elastic-perfectly plastic contact theory cannot perfectly reflect the above mechanical process. Therefore, on basis of the classical Hertz contact theory, the damage of the rock-shed roof induced by the rockfall is firstly introduced to consider its effect on the material elastic modulus, and then the revised Hertz contact theory considering the damage is proposed. Secondly, in view of the existing calculation method of the maximum rockfall impact force based on the theorem of impulse, a new calculation method is proposed by combining the revised Hertz contact theory. Thirdly, according to the dynamic mechanical response process of the rock-shed roof under the rockfall and in view of the revised Hertz contact theory, a dynamic damage model for the rock-shed roof under the rockfall is proposed, which can perfectly illustrate the variation law of the impact force with the deformation of the rock-shed roof during the rockfall. Finally, the proposed model is verified with other models for the maximum rockfall impact force. In all, the proposed model can perfectly describe the dynamic mechanical behavior of the rock-shed roof under the rockfall, which can be referred for the engineering design.

Key words rockfall • impact force • the rock-shed roof • a dynamic damage model • Hertz contact theory

Declarations

Funding

This study is supported by the National Key Research and Development Plan of China (Grant No：2019YFC1509701).

Conflict of interest/Competing interests

The authors declare that they have no conflict of interest.

Availability of data and material

Not applicable

Code availability

Not applicable

Authors' contributions

Not applicable

Ethics approval

I certify that this manuscript is original and has not been published and will not be submitted elsewhere for publication while being considered by Natural Hazards. And the study is not split up into several parts to increase the quantity of submissions and submitted to various journals or to one journal over time. No data have been fabricated or manipulated (including images) to support the conclusions. No data, text, or theories by others are presented as if they were our own.

Consent to participate

Not applicable

Consent for publication

The author agrees to publication in Natural Hazards.

1 Introduction

In many mountainous areas, rockfall has become the most serious and frequent geological hazard except for the landslides. Because of the high speed, suddenness, randomness and kinetic energy, rockfall poses a serious threat to many infrastructures and buildings even casualties, and therefore it attracts much attention to predict its movement trajectories and control measures (Bunce et al., 1997; Volkwein et al., 2011; Li and Lan, 2015; Ferrari et al., 2016; Zhu et al., 2019). In practice, many types of rockfall protection structures are designed to reduce the disasters induced by the rockfall such as embankment (Lambert and Bourrier, 2013), rock-shed (Ouyang et al, 2019; Zhao et al, 2018), flexible net (Yang et al., 2019; Zhao et al., 2020) and pile-plate retaining wall (Hu et al., 2019). Among them, the rock-shed is one of the important structures for reducing damage from rockfall on roads and railways, which is constructed by the reinforced concrete with backfilled gravel soil cushions on its top (Kawahara and Muro, 2006). The role of the latter is to absorb the rockfall impact energy to reduce the impact force on the underlying reinforced concrete. However, the destruction of the rock-shed roof often occurs due to the rockfall, shown as Fig.1 (Wyllie, 2014).

Therefore, it is very significant to conduct the study on the dynamic response of the rock-shed structure under the rockfall for its design. Many researches have been done in this field, which can be classified into the following three aspects namely model or field experiment, theoretical model and numerical simulation. First of all, many researchers have conducted the relevant experiments. Pichler et al. (2005) designed the rockfall experiments to study the relations between the penetration depth, the impact duration, the impact force and the rock boulder mass, fall height and the indentation resistance of the gravel. Calvetti (2011) conducted the real scale tests to evaluate the rockfall impact force acting at the boulder-soil interface and the dynamic excitation of the sheltering tunnel. Calvetti and Prisco (2012) conducted a series of rockfall tests on a sheltering tunnel, in which the rockfall is a reinforced-concrete sphere with mass 850kg, diameter 0.9m dropping from 5~45m high. The impact force and its deflection of the shelter are studied. Zhao et al. (2021) conducted a systematic experiment to study the ability of two kinds of composite cushion in protecting the rock-shed under multiple rockfalls. It shows that the sand-EPE (expandable polyethylene) composite cushion is much better than the sand-EPS (expandable polystyrene) one in the multi-impact resistance and durability, and is more suitable to protect the rock-shed in practical engineering. Second, in view of the theoretical study, the existing theoretical models for the rockfall impact force on the reinforced-concrete structure are mainly derived from the classic Hertz contact theory which is based on the elastic mechanics. However, the structure will exhibit the plastic deformation, therefore many researchers have made

some improvements to it. Thornton et al. (1997; 1998; 2013) suggested that the normal interaction becomes plastic when a 'limiting contact pressure' reached at the center of the contact area, which originated from Hardy et al. (1971). Vu-Quoc et al. (1999; 2000) proposed an accurate model for the normal force-displacement relation for contacting spherical particles by accounting for the effects of plastic deformation. By considering the strengthening coefficient of the gravel soil, Wang et al. (2020) proposed a theoretical calculation method of the rockfall impact force and penetration depth. Meanwhile the dynamic response of the rock-shed roof under the rockfall is related to not only the rockfall characteristic but also the mechanical property of the rock-shed roof. Therefore, many scholars proposed the dynamic model for the rock-shed roof under the rockfall by combining the Hertz contact theory and rock-shed roof. Olsson (2003; 2010) set up an analytical model for delamination of the orthotropic laminated composite plates under small mass impact based on Hertz contact theory. With the elasto-plastic contact theory, Zheng and Binienda (2007) derived the closed-form approximations of the contact force, indentation and plate central displacement for the impact loading of composite laminates. Finally, many studies have been conducted with the numerical simulation. Yan et al. (2018) used LS-DYNA code to analyze the impact force and dynamic response of the reinforced concrete slab by considering the falling rock's shape and impact angle. Shen et al. (2019) investigated the mechanism of rockfall impact against a granular soil buffering layer above a concrete/rock shed by discrete element method, which indicates that the maximum impact force increases linearly with the rockfall sphericity. Naito et al. (2020) used a discrete element method to investigate the cushioning performance of a sand cushion and proposed the effective and rational measures for the protection of the rock-shed.

However although many studies have been conducted on this issue, there are still two problems to solve. One is that the dynamic response of the rock-shed roof is an evident dynamic process which can be divided into three stages namely elastic compression stage at the early stage of the collision, plastic deformation stage when the stress of the rock-shed roof induced by the rockfall exceeds its yield strength, and the elastic resilience stage after the maximum compression deformation reaches. Although the study by Zheng and Binienda (2007) is also conducted according to these three stages, they assumed that the elastic modulus of the rock-shed roof was invariable at the second stage which was unreasonable. Because during the plastic deformation stage, the elastic modulus will decrease with increasing its plastic deformation. The other one is that only the variation of the impact force on the rock-shed roof with time is given, but the variation of the impact force with the rock-shed roof deformation is not given (Zheng and Binienda, 2007; Olsson, 2003; Olsson, 2010). Therefore, it is impossible to

obtain the permanent deformation of the rock-shed roof under the rockfall, which is not conducive to the safety assessment of the rock-shed in the future.

For these two issues above, on basis of the classic Hertz contact theory, the revised Hertz contact theory is firstly proposed by considering the rock-shed roof damage induced by the rockfall. Next, according to the dynamic response process of the rock-shed roof under the rockfall, the dynamic damage model for the rock-shed roof is proposed, and the determination method of the model's parameters are discussed. Finally, its application and validity are made with the calculation examples.

2 Hertz contact theory and its improvement

Fig.2 depicts the contact between two spheres subjected to normal force P (Hertz, 1882). The normal pressure $p(r)$ on the contact surface can be expressed as

$$p(r)=\frac{3P}{2\pi a^2}\left[1-\left(\frac{r}{a}\right)^2\right]^{1/2} \tag{1}$$

where, a is the radius of the contact area, $r(0 \leqq r \leqq a)$ is the distance from the center of the contact area to any point of the contact area, P is the contact force.

Therefore, the maximum normal pressure $p_{\max}$ at r=0 can be expressed as

$$p_{\max}=\frac{3P}{2\pi a^2} \tag{2}$$

The contact deformation is composed of the following two parts.

$$\delta=\delta_1+\delta_2 \tag{3}$$

where, δ_1 and δ_2 are the deformations of these two contact spheres respectively.

The relationship between the contact deformation and the contact area is

$$a^2=R\delta \tag{4}$$

where, R is the equivalent radius, $\frac{1}{R}=\frac{1}{R_1}+\frac{1}{R_2}$, R_1 and R_2 are the radii of these two contact spheres respectively.

The relationship between the contact force P and the contact deformation δ can be expressed as (Hertz, 1882)

$$P=\frac{4}{3}ER^{\frac{1}{2}}\delta^{\frac{3}{2}} \tag{5}$$

where, E is the equivalent elastic modulus, $\frac{1}{E}=\frac{1-\mu_1^2}{E_1}+\frac{1-\mu_2^2}{E_2}$, E_1, μ_1, E_2 and μ_2 are the elastic moduli and Poisson's ratio of these two contact bodies respectively.

The abovementioned Hertz contact theory is only suitable for the material in the elastic stage, therefore the contact force obtained with it is always rather large in the practical engineering. This is because the plastic deformation will occur in the material when the contact compressive stress exceeds the material's yield strength, so the classic Hertz contact theory is unsuitable. In view of this, many improvements have been made which can be classified into the following two models, e.g. Hertz plastic contact theory and Hertz damage contact theory. As for the former, Thornton (1997; 1998) proposed the Hertz plastic contact theory by introducing the perfectly elasto-plastic model into the classic Hertz contact theory, with which the prediction is in more agreement with the practical one. Meanwhile with the development of the damage mechanics, many researchers begin to introduce it into the classic Hertz contact theory. For instance, Travares and King (2002) and Travares (2002) set up the impact damage model for the spherical particles according to their force-deformation characteristic under impact loading on basis of the classic Hertz contact theory and continuum damage theory.

$$P=\frac{d^{0.5}}{3}\tilde{K}\delta^{\frac{3}{2}}=\frac{d^{0.5}}{3}K\left(1-D\right)\delta^{\frac{3}{2}} \tag{6}$$

where, d is the diameter of the spherical particle, K and $\tilde{K}$ are the initial and effective stiffness of the spherical particle respectively, D is the damage of the spherical particle induced by impact loading, which is defined as

$$D=\left(\frac{\delta}{\delta_c}\right)^{\gamma} \tag{7}$$

where, δ_c is the compression deformation of the spherical particle when the impact failure occurs, when $\delta=\delta_c$, $D=1$. γ is the impact damage index.

It can be seen from Eq.(7) that the spherical particle's any contact deformation induced by impact loading will lead to damage. However, according to the classic Hertz contact theory, when the spherical particle's contact deformation δ is less than its yield deformation δ_y, the spherical particle is in the elastic contact condition with no damage occurs, namely $D=0$. It is evident that Eq.(7) cannot describe this condition, which is its deficiency.

Because the rock and reinforced concrete are the natural damage materials, the collision between them will inevitably lead to the occurrence, propagation and coalescence of the microcracks which will lead to the deterioration of their physical and mechanical property, even failure. Therefore, the damage induced by collision

153 can be defined as the deterioration of the elastic modulus. The typical force-deformation under collision can be
154 divided into the four stages, e.g. the initial collision one, elastic collision one, plastic damage collision one and
155 unloading resilience one. Because the first stage is short, it is often ignored. At the second stage, the
156 force-deformation between the particles fits with the classic Hertz contact theory, and accordingly no damage
157 occurs. When the contact stress exceeds the particle's initial yield strength, the force-deformation curve will be not
158 linear any more, and the damage occurs, which is the third stage. When the contact force reaches the peak, the
159 fourth stage will begin, in which the particle's deformation is elastic and the damage keeps constant. Therefore,
160 the particle's damage D can be defined as

161
$$D=1-\frac{\bar{E}}{E}=\begin{cases} 0 & \delta \le \delta_y \\ \left(\dfrac{\delta-\delta_y}{\delta_c-\delta_y}\right)^{\gamma} & \delta_y < \delta \le \delta_m \end{cases} \tag{8}$$

162 where, $\bar{E}$ and E are the particle's effective and initial elastic modulus. δ_y, δ_m and δ_c are the contact deformation
163 at the initial yield of the particle, the maximum contact deformation and the contact deformation when the particle
164 completely fails, therefore $\delta_y<\delta_m \leqq \delta_c$ satisfies.

165 So the relation between the contact stress and contact deformation considering the material damage is

166
$$P=\frac{4}{3}E(1-D)R^{\frac{1}{2}}\delta^{\frac{3}{2}} \tag{9}$$

167 # 3 The dynamic response of the rock-shed roof under the rockfall

168 ## 3.1 Impact force induced by the rockfall on the rock-shed roof

169 Assume the rockfall is a moving mass point with velocity v_0, and the rock-shed roof is a stationary plane
170 without overlying buffer material, the corresponding model is shown as Fig.3.

171 The total velocity of the rockfall can be decomposed into the horizontal and vertical components as follows.

172
$$v_x=v_0\cos\theta\,,\quad v_y=v_0\sin\theta \tag{10}$$

173 where, v_0, v_x and v_y are the rockfall total velocity, horizontal and vertical velocity components respectively at the
174 moment the rockfall reaches the rock-shed roof. θ is the impact angle.

175 Because the failure of the roof is induced mainly by the vertical impact, only the vertical impact by the
176 rockfall is considered here. According to Newton's second law, there is

$$P = m_1 \frac{dv_1}{dt} = -m_2 \frac{dv_y}{dt} \tag{11}$$

where, m_1 and m_2 are the masses of the rock-shed roof and rockfall respectively, v_1 is the movement velocity of the rock-shed roof, g is the gravitational acceleration, and P is the impact force on the rock-shed roof by the rockfall.

From Eq.(11), we obtain

$$-\frac{\left(m_1+m_2\right)P}{m_1 m_2} = \frac{d\left(v_y - v_1\right)}{dt} = \frac{d^2\delta}{dt^2} \tag{12}$$

Combining Eqs.(5) and (12) yields

$$\frac{d^2\delta}{dt^2} = -\frac{4}{3m} E R^{\frac{1}{2}} \delta^{\frac{3}{2}} \tag{13}$$

where, m is the equivalent mass, $\frac{1}{m} = \frac{1}{m_1} + \frac{1}{m_2}$.

Integrating δ and with the initial conditions $\delta\big|_{t=0} = 0$, $\delta'\big|_{t=0} = v_0 \sin\theta$, we obtain

$$\frac{1}{2}\left[\left(v_0 \sin\theta\right)^2 - \left(\frac{d\delta}{dt}\right)^2\right] = \frac{8}{15m} E R^{\frac{1}{2}} \delta^{\frac{5}{2}} \tag{14}$$

When $\delta=\delta_{max}$, $\frac{d\delta}{dt} = 0$, substituting it into Eq.(14) yields

$$\delta_{\max} = \left[\frac{15m\left(v_0 \sin\theta\right)^2}{16 E R^{\frac{1}{2}}}\right]^{\frac{2}{5}} \tag{15}$$

Substituting Eq.(15) into Eq.(5), we obtain the maximum impact force P_{max0} induced by the rockfall on the rock-shed roof.

$$P_{\max 0} = \frac{4}{3} E^{\frac{2}{5}} R^{\frac{1}{5}} \left[\frac{15m\left(v_0 \sin\theta\right)^2}{16}\right]^{\frac{3}{5}} \tag{16}$$

When the effect of the material damage induced by the rockfall is considered, the revised maximum impact force P_{max} of the rockfall on the rock-shed roof can be obtained by substituting Eq.(8) into Eq.(16).

$$P_{\max} = \frac{4}{3}\left[E\left(1-D\right)\right]^{\frac{2}{5}} R^{\frac{1}{5}} \left[\frac{15m\left(v_0 \sin\theta\right)^2}{16}\right]^{\frac{3}{5}} \tag{17}$$

3.2 The dynamic mechanical response of the rock-shed roof

The engineering practice indicates that the rockfall impact force will cause some damage to the rock-shed roof, so the Hertz contact theory considering damage is more reasonable.

From the previous studies, the relation between the impact force and deformation of the rock-shed roof under the rockfall can be divided into the following three stages (Olsson, 2010; Zheng and Binienda, 2007).

① Stage I: the linear loading stage at the initial collision

At the initial stage of collision, the impact force induced by the rockfall on the rock-shed roof is small, and accordingly the deformation of the rock-shed roof is also little. So it is in the elastic deformation condition, and the contact force between them satisfy the classic Hertz contact theory, namely

$$P(\delta)=\frac{4}{3}ER^{\frac{1}{2}}\delta^{\frac{3}{2}} \qquad \left(0\le\delta\le\delta_y\right) \tag{18}$$

where, δ_y is the deformation of the rock-shed roof when the initial yield occurs.

② Stage II: the damage loading stage

With the impact loading continuing, the impact force and deformation of the rock-shed roof both increase. When the impact force exceeds the rock-shed roof yield strength, the plastic deformation will produce in the rock-shed roof and accordingly the damage occurs. Therefore, the impact force should satisfy the revised Hertz contact theory considering damage, namely

$$P(\delta)=2E(1-D)R^{\frac{1}{2}}\delta_y^{\frac{1}{2}}\left(\delta-\delta_y\right)+\frac{4}{3}E(1-D)R^{\frac{1}{2}}\delta_y^{\frac{3}{2}} \qquad \left(\delta_y\le\delta\le\delta_m\right) \tag{19}$$

where, δ_m is the maximum deformation of the rock-shed roof.

③ Stage III: the unloading stage

When the deformation of the rock-shed roof reaches the maximum, the rockfall velocity will decrease to zero, and then the elastic deformation energy stored in the rock-shed roof will release and its resilience deformation will happen. During this stage, no new damage occurs in the rock-shed roof, but the existing damage will not recover any more. So the rock-shed roof elastic modulus is the same as that at its maximum deformation, and accordingly its relation between the contact force and deformation is

$$P(\delta)=2E(1-D_m)R^{\frac{1}{2}}\delta_y^{\frac{1}{2}}\left(\delta_m-\delta_y\right)+\frac{4}{3}E(1-D_m)R^{\frac{1}{2}}\left(\delta^{\frac{3}{2}}-\delta_m^{\frac{3}{2}}+\delta_y^{\frac{3}{2}}\right) \qquad \left(\delta\le\delta_m\right) \tag{20}$$

where, D_m is the maximum damage of the rock-shed roof corresponding to its maximum deformation δ_m before unloading.

When unloading completes, the contact force $P(\delta)$ should be the rockfall gravity m_2g, and then the corresponding residual deformation δ_0 of the rock-shed roof can be obtained with Eq.(20). It is the plastic deformation of the rock-shed roof induced by the rockfall.

3.3 Determination of the parameters in the proposed model

When the proposed model is adopted to analyze the dynamic response of the rock-shed roof under the rockfall, the parameters δ_y and δ_m must be determined first.

(1) Determination of δ_y

The deformation δ_y of the rock-shed roof is corresponding to its initial yield strength σ_{py}, which can be obtained with the material mechanics test. On basis of Hertz contact theory, Vu-Quoc et al. (1999; 2000) assumed that when Von Mises yield criterion satisfies, the relation between the contact force P_y induced by the rockfall on the rock-shed roof and its yield strength σ_{py} is

$$P_y = \left(A_y\right)^3 \frac{\pi^3 R^2 \left(1-\mu^2\right)^2}{6E^2} {\sigma_{py}}^3 \tag{21}$$

where, E and μ are the material's elastic modulus and Poisson's ratio respectively, A_y is the material constant related to μ, and it is 1.61 and 1.74 when μ is 0.3 and 0.4, respectively.

Meanwhile, the material's initial yield point is the junction of the elastic stage and plastic damage stage, therefore it belongs to these two stages at the same time. So P_y can be solved with material's yield strength, and then the corresponding deformation δ_y of the rock-shed roof can be solved with Eq.(5).

(2) Determination of δ_m

It can be known that the maximum impact force of the rock-shed roof and its maximum deformation occur at the same time, therefore from Eqs.(17) and (19), we obtain

$$P_{\max} = P\left(\delta\right)\Big|_{\delta=\delta_m} \tag{22}$$

Then we can obtain an equation about δ_m (where δ_c is the material impact deformation corresponding to its complete failure, and it can be obtained with experiment.), from which δ_m can be obtained by iterative solution.

4 Analysis of the calculation example

4.1 Description of the calculation example

The calculation model is shown in Fig.3. Assume the velocity and its angle of the spherical rockfall are v_0 and θ respectively at the moment it reaches the rock-shed roof. The rock-shed roof and rockfall are supposed to be C20 reinforced concrete and granite respectively, whose calculation parameters are show in Tab.1. Because the mass of the rock-shed roof is much larger than that of the rockfall, namely $m_1>>m_2$, therefore, the equivalent mass is about the rockfall mass, namely $m\approx m_2$.

4.2 Analysis of the calculation results

The calculation procedure and results are as follows.

① Stage I: the linear loading stage at the initial collision

According to the calculation parameters shown in Tab.1, the impact force P_y leading to the yield of the rock-shed roof is firstly solved to be 0.603MN with Eq.(21), that is to say its maximum elastic force is 0.603MN. Then its corresponding deformation δ_y is solved to be 1.39mm with Eq.(18). Therefore, the deformation of the rock-shed roof under the rockfall linearly increases from 0 to 1.39mm, and the corresponding contact force linearly increases from 0 to 0.603MN.

② Stage II: the damage loading stage

Firstly, according to Eqs.(18), (19) and (22), the maximum deformation δ_m of the rock-shed roof under the rockfall is solved to be 15.42mm. Then some points of δ between δ_y~δ_m are taken, and the corresponding contact force $P(\delta)$ can be solved with Eq.(19). Finally, the damage loading curve of the rock-shed roof can be drawn with these results.

③ Stage III: the unloading stage

Firstly, the damage of the rock-shed roof corresponding to the its maximum deformation δ_m is solved to be 0.0578 here. Substituting it into Eq.(20) and assuming the rockfall impact force $P(\delta)$ to be m_2g, the corresponding permanent deformation δ_0 of the rock-shed roof is 10.56mm. Then some points of δ between δ_m~δ_0 are taken, and the corresponding contact force $P(\delta)$ can be solved with Eq.(20). Finally, the unloading curve of the rock-shed roof can be drawn with these results.

Then the relation of the impact force on the rock-shed roof induced by the rockfall with its damage and deformation is shown in Fig.4. It can be seen that it can be divided into three stages, e.g. the linear loading stage, the damage loading stage and the unloading stage. During the first stage, the rock-shed roof produces elastic deformation, namely its impact force induced by the rockfall is linear with its deformation. When the impact force increases to the yield strength of the rock-shed roof, it will go into the damage loading stage. It is found from the

276 slope of the curve that the slope of the damage loading stage is larger than that of the elastic loading stage, which
277 indicates that the reinforced concrete will exhibit a plastic strengthening phenomenon after it goes into the plastic
278 deformation. At the peak of the impact force, the rockfall velocity reduces to zero. After that the unloading
279 resilience of the rock-shed roof begins, and the elastic deformation component gradually recovers in which the
280 rockfall impact force and total deformation of the rock-shed roof both gradually decreases. When the rockfall
281 impact force reduces to zero, the corresponding deformation of the rock-shed roof is its permanent deformation
282 namely the residual plastic deformation. Meanwhile, it can be seen from the damage-deformation curve that the
283 damage only occurs at the stage II and its maximum damage is only 0.0578. It shows that the damage of the
284 rock-shed roof induced by the rockfall is little in this calculation example. However it is noted from Eq.(7) that the
285 damage of the rock-shed roof is related to δ_c and γ, and the accurate description of the damage evolution greatly
286 depends on the accurate determination of these two above damage parameters.

287 ## 4.3 parametric sensitivity analysis

288 It can be seen from the proposed model that the dynamic response of the rock-shed roof under the rockfall is
289 related to not only its physical and mechanical property but also the parameters of the rockfall to large extent.
290 Therefore, the parametric sensitivity analysis is adopted to study the effect of the parameters of the rockfall and
291 rock-shed roof on the calculation results.

292 (1) Effect of the rockfall velocity

293 The rockfall velocity is assumed to be 2, 3, 4 and 5m/s, and the other parameters are as shown in Tab.1. The
294 following conclusions can be obtained from Fig.5. First of all, with increasing the rockfall velocity, the maximum
295 deformation of the rock-shed roof increases from 5.27mm to 8.3, 11.61 and 15.42mm respectively, and
296 accordingly the corresponding maximum impact force on the rock-shed roof also increases from 3.12MN to 5.07,
297 7.12 and 9.15MN respectively. It indicates that the impact force and deformation of the rock-shed roof induced by
298 the rockfall is linear to the rockfall velocity. Secondly, with increasing the rockfall velocity, the residual
299 deformation of the rock-shed roof increases from 2.47mm to 4.80, 7.39 and 10.56mm respectively. It indicates that
300 the plastic deformation of the rock-shed roof increases with the rockfall velocity, which shows that the total
301 damage of the rock-shed roof induced by the rockfall increases. Finally, the rockfall velocity does not change the
302 linear stage of the curve, this is because it is determined by both the material yield strength and Hertz contact
303 theory, and not affected by the rockfall velocity. It agrees with the conclusions obtained by other researcher (Ning,

1995). However it is noted that the material yield strength is assumed to be not related to the rockfall, which agrees with the practical condition when the rockfall velocity is small. However, when the rockfall velocity is large, the more evident dynamic response of the rock-shed roof under the rockfall will occur, and accordingly the material dynamic yield strength will increase with the load strain rate. But its increase extent is much related to the material mechanical property, which should be tested with the experiment (Kumar, 1968).

(3) Effect of the rockfall radius

The rockfall radius is assumed to be 0.25, 0.5, 0.75 and 1m, accordingly the corresponding rockfall mass is 164, 1309, 4418 and 10472kg, and the other parameters are as shown in Tab.1. The following conclusions can be obtained from Fig.6. First of all, with increasing the rockfall radius, the maximum deformation of the rock-shed roof increases from 3.74mm to 7.47, 11.27 and 15.42mm respectively, and accordingly the corresponding maximum impact force on the rock-shed roof also increases from 0.59MN to 2.34, 5.25 and 9.15MN respectively. It indicates that the impact force and deformation of the rock-shed roof induced by the rockfall is linear to the rockfall radius. Secondly, with increasing the rockfall radius, the residual deformation of the rock-shed roof increases from 2.53mm to 5.0, 7.65 and 10.56mm respectively. It indicates that the plastic deformation of the rock-shed roof increases with the rockfall radius, which shows that the total damage of the rock-shed roof induced by the rockfall increases. However, it is noted that the damage evolution of the rock-shed roof is assumed to be the same, namely the damage parameters δ_c and γ in Eq.(9) are assumed to be constant under different conditions, which will inevitably lead to some error.

(3) Effect of the damage parameter of the roof

In the proposed method, δ_c and γ are two important damage parameters, whose effect on the calculation results are shown in Fig.7. The following conclusions can be obtained. First of all, with increasing δ_c, the impact force-deformation curve of the rock-shed roof has some difference, but its extent is little. When δ_c increases from 25mm to 30, 35 and 40mm, the maximum impact deformation of the rock-shed roof only decreases from 16.71mm to 15.42, 15.17 and 15.05mm, and accordingly the corresponding maximum impact force only increases from 8.67MN to 9.15, 9.26 and 9.31MN respectively. Meanwhile, the residual deformation of the rock-shed roof only decreases from 11.66mm to 10.56, 10.40 and 10.30mm respectively, which indicates that the increase in δ_c has little effect on the dynamic response of the rock-shed roof. Moreover, it can be seen from Fig.7(a) that only the curve with δ_c=25mm has much difference with other three ones, which indicates that the effect of δ_c on the calculation results is little when it increases to some extent. Secondly, with γ increasing from 2 to 3, 4 and 5, the maximum deformation the rock-shed roof gradually decreases from 16.41mm to 15.34, 15.05 and 14.96mm

respectively, and the corresponding maximum impact force gradually increases from 8.77MN to 9.19, 9.31 and 9.35MN respectively. Meanwhile the residual deformation of the rock-shed roof decreases from 11.41mm to 10.49, 10.30 and 10.20mm respectively, which indicates that the effect of γ on the dynamic response of the rock-shed roof firstly increases rapidly, and then the increase extent decreases.

5 Verification of the proposed model

In order to validate the proposed model, the calculation models of the maximum rockfall impact force proposed by Labiouse et al. (1966), Kawahara et al. (2006), Pichler et al. (2006) and Hertz (1882) namely Eqs.(23), (24), (25) and (5) are adopted here.

The model proposed by Labiouse et al. (1966) is

$$P_{\max} = 1.765 M_E^{2/5} R^{1/5} \left(WH\right)^{3/5} \tag{23}$$

where, $P_{\max}$ is the maximum impact force (kN), M_{E} is the modulus of subgrade obtained from a standardized plate bearing test on the soil cushion (kPa); R is the radius of the rockfall part in contact with the soil cushion (m), W is the weight of the rockfall (kN), H is the falling height of the rockfall (m).

The model proposed by Kawahara et al. (2006) is

$$P_{\max} = 2.108 \lambda^{2/5} \left(Mg\right)^{2/3} H^{3/5} \tag{24}$$

where, λ is the Lame's constant (kPa), M is the weight mass (t), g is the gravitational acceleration (m/s^2), H is the falling height of the rockfall (m).

The model proposed by Pichler et al. (2006) is

$$P_{\max} = 2Mv/\Delta t \tag{25}$$

where, M, v and Δt are the rockfall weight mass (kg), velocity (m/s) and impact loading time (s), respectively.

The following conclusions can be drawn from Fig.8. First of all, the impact force increases nonlinearly with the rockfall radius (or rockfall mass), especially when the rockfall radius is rather large, the rockfall maximum impact force increases rapidly with the rockfall radius. Second, in view of the magnitude of the rockfall impact force, the calculation result of the proposed model is between that of the other four models. Meanwhile it is much closer to that of Hertz (1882) and Labiouse et al. (1966), however their gap becomes larger with increasing the rockfall radius. Take the rockfall radius r=1m for instance, the results of Hertz (1882) and Labiouse et al. (1966) are much closer, which are 11.50 and 11.03MN respectively. However, the results of Kawahara et al. (2006) and

Pichler et al. (2006) are much closer, which are 2.13 and 3.74MN respectively. The result of the proposed model is 9.15MN, which is much closer to that of Hertz (1882) and Labiouse et al. (1966), and the errors between them are 17.04% and 20.43% respectively. While, the results of Kawahara et al. (2006) and Pichler et al. (2006) are 4.30 and 2.45 times that of the proposed model. Finally, it is noted that some calculation parameters in these models are difficult to accurately test, and therefore they are adopted by experience. It will lead to some errors which is also a main reason leading to the result shown in Fig.8. In the future, the selection of these parameters in these models should be studied further. In all, it can be seen from Fig.8 that the proposed model for the rock-shed roof under the rockfall is reasonable.

6 Conclusions

For the shortcoming that the classic elastic Hertz contact theory cannot consider the damage of the material induced by collision, this research firstly proposes the revised Hertz contact theory by considering the material damage. And then on basis of the existing study, the revised calculation method of the rockfall maximum impact force on the rock-shed roof is proposed by taking into account the material damage. Finally, according to the dynamic response of the rock-shed roof under the rockfall, the dynamic damage model for the rock-shed roof under the rockfall is proposed. The revised Hertz contact theory by considering the damage and the dynamic model for the rock-shed roof under the impact loading are not new indeed. However, without the incorporating, these models alone cannot yield the completely dynamic force–deformation relations of the rock-shed roof. The proposed model can perfectly capture the dynamic response of the rock-shed roof under the rockfall.

The proposed model is validated by the comparison with other methods, which indicates that it can reasonably determine the variation of the rockfall impact force with the deformation of the rock-shed roof. The influence of the rockfall velocity, radius and damage parameters on the dynamic behavior of the rock-shed roof are accordingly studied. Overall, the proposed model provides a way to simulate the dynamic behavior of the rock-shed roof under the rockfall.

References

Bunce CM, Cruden D, Morgenstern N (1997) Assessment of the hazard from rock fall on a highway. Can Geotech J 34: 344–356

Calvetti F (2011) Rockfall shelters covered by granular layers. Eur J Environ Civ En 15(S1): 73-100

Calvetti F, Di Prisco C (2012) Rockfall impacts on sheltering tunnels: real-scale experiments. Géotechnique

62(10): 865-876

Ferrari F, Giacomini A, Thoeni K (2016) Qualitative Rockfall Hazard Assessment: A comprehensive review of current practices. Rock Mech Rock Eng 49: 2865-2922

Hardy C, Baronet CN, Tordion GV (1971) The elasto-plastic indentation of a half-space by a rigid sphere, Int J Numer Meth Eng 3: 451–462

Hertz H (1882) Über die Berührung fester elastischer Körper. J Reine Angew Math 92: 156-171

Hu XW, Mei XF, Yang Y, Luo G, Wu JL (2019) Dynamic response of pile-plate rock retaining wall under impact of rockfall. J Eng Geol 27(1): 123-133 (in Chinese)

Kawahara S, Muro T (2006) Effects of dry density and thickness of sandy soil on impact response due to rockfall. J Terramechanics 43(3): 329-340

Kumar A (1968) The effect of stress rate and temperature on the strength of basalt and granite. Geophysics 33(3): 501-510

Labiouse V, Descoeudres F, Montani S (1966) Experimental Study of rock Sheds Impacted by rock Blocks. Struct Eng Int 6(3): 171-175

Lambert S, Bourrier F (2013) Design of rockfall protection embankments: A review. Eng Geol 154: 77-88

Li LP, Lan HX (2015) Probabilistic modeling of rockfall trajectories: a review. B Eng Geol Environ 74(4): 1163-1176

Naito N, Maeda K, Konno H, Ushiwatari Y, Suzuki K, Kawase R (2020) Rockfall impacts on sand cushions with different soil mechanical characteristics using discrete element method. Soils Found 60(2): 384-397

Ning Z (1995) Elasto-plastic impact of fine particles and fragmentation of small agglomerates [PhD thesis] University of Aston in Birmingham

Olsson R (2003) Closed form prediction of peak load and delamination onset under small mass impact. Compos Struct 59(3): 341-349

Olsson R (2010) Analytical model for delamination growth during small mass impact on plates. Int J Solids Struct 47(21): 2884-2892

Ouyang CJ, Liu Y, Wang DP, He SM (2019) Dynamic analysis of rockfall impacts on geogrid reinforced soil and EPS absorption cushions. KSCE J Civ Eng 23(1): 37-45

Pichler B, Hellmich Ch, Mang H A (2005) Impact of rocks onto gravel design and evaluation of experiments. Int J Impact Eng 31(5): 559-578

Pichler B, Hellmich C, Mang H A, Eberhardsteiner J (2006) Loading of a gravel-buried steel pipe subjected to rockfall. J Geotech Geoenviron 132(11): 1465-1473

Shen WG, Zhao T, Dai F, Jiang MJ, Zhou GGD (2019) DEM analyses of rock block shape effect on the response of rockfall impact against a soil buffering layer. Eng Geol 249: 60-70

Tavares LM, King RP (2002) Modeling of particle fracture by repeated impacts using continuum damage mechanics. Powder Technol 123(2/3): 138-146

Tavares LM (2002) Analysis of particle fracture by repeated stressing as damage accumulation Powder Technol 123(2/3): 138-146

Thornton C (1997) Coefficient of restitution for collinear collisions of elastic–perfectly plastic spheres. Trans ASME J Appl Mech 64: 383–386.

Thornton C, Cummins SJ, Cleary PW (2013) An investigation of the comparative behavior of alternative contact force models during inelastic collision. Powder Technol 233: 30-46

Thornton C, Ning Z (1998) A theoretical model for the stick/bounce behaviour of adhesive, elatsic-plastic spheres. Powder Technol 99(2): 154-162

Volkwein A, Schellenberg K, Labiouse V, Agliardi F, Berger F, Bourrier F, Dorren LKA, Gerber W, Jaboyedoff M (2011) Rockfall characterisation and structural protection - a review. Nat Hazard Earth Sys 11: 2617-2651

Vu-Quoc L, Zhang X, Lesburg L (2000) A normal force-displacement model for contacting spheres accounting for plastic deformation: Force-driven formulation. J Appl Mech-Trans ASME 67(2): 363-371

Vu-Quoc L, Zhang X (1999) An elastoplastic contact force-displacement model in the normal direction: displacement-driven version. P Roy Soc A-Math Phy 455: 4013-4044

Wang YS, Xu M, Yang C, Lu MY, Meng J, Wang ZL, Wang MN (2020) Effects of elastoplastic strengthening of gravel soil on rockfall impact force and penetration depth. Int J Impact Eng 136: 103411

Wyllie DC (2014) Rock Fall Engineering, CRC Press, Taylor and Francis Group, pp. 121-123

Yan P, Zhang JH, Fan Q, Zhang YD (2018) Numerical simulation of the effects of falling rock's shape and impact pose on impact force and response of RC slabs. Constr Build Mater 160: 497-504

Yang JJ, Duan SL, Li QF, Liu CQ (2019) A review of flexible protection in rockfall protection. Nat Hazards 99(1): 71-89

Zhao L, Yu ZX, Liu YP, He JW, Chan SL, Zhao SC (2020) Numerical simulation of responses of flexible rockfall barriers under impact loading at different positions. J Constr Steel Res 167: 105953

Zhao P, Xie LZ, Li LP, Liu Q, Yuan S (2018) Large-scale rockfall impact experiments on a RC rock-shed with a

448 newly proposed cushion layer composed of sand and EPE. Eng Struct 175: 386-398
449 Zhao P, Yuan S, Li LP, Ge Q, Liu J, Du LH (2021) Experimental study on the multi-impact resistance of a
450 composite cushion composed of sand and geofoam. Geotext Geomembranes 49(1): 45-56
451 Zheng D, Binienda WK (2007) Effect of permanent indentation on the delamination threshold for small mass
452 impact on plates. Int J Solids Struct 44: 8143-8158
453 Zhu C, Tao ZG, Yang S, Zhoa S (2019) V shaped gully method for controlling rockfall on high-step slopes in
454 China. B Eng Geol Environ 78: 2731-2747

Figures

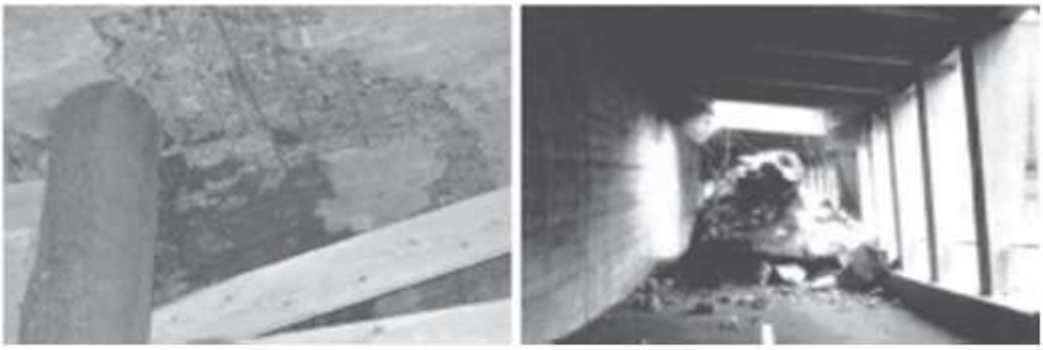

Figure 1

Damages of the rock-shed due to rockfall

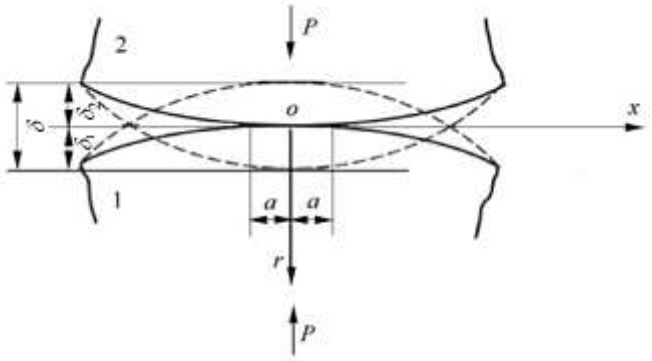

Figure 2

Contact problem of Hertz of two spheres. a is the radius of the contact area, P is the contact force, δ1 and δ2 are the deformations of these two contact spheres respectively.

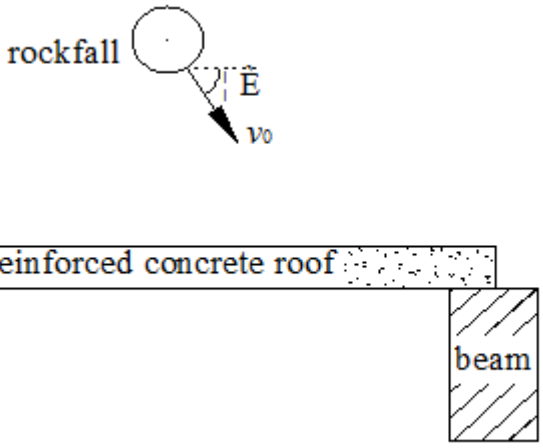

Figure 3

The model for the rock-shed roof under the rockfall. The velocity and its angle of the rockfall are v0 and θ respectively. The rock-shed roof is made of reinforced concrete and it can be seen to be fixed at two ends.

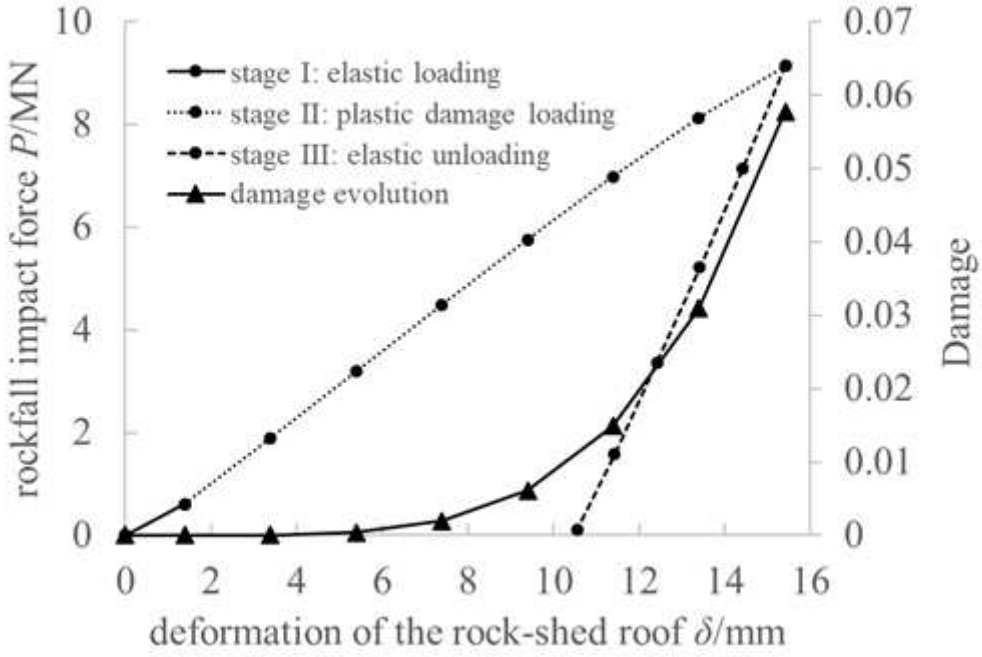

Figure 4

The impact force-deformation curve of the reinforced concrete under the rockfall

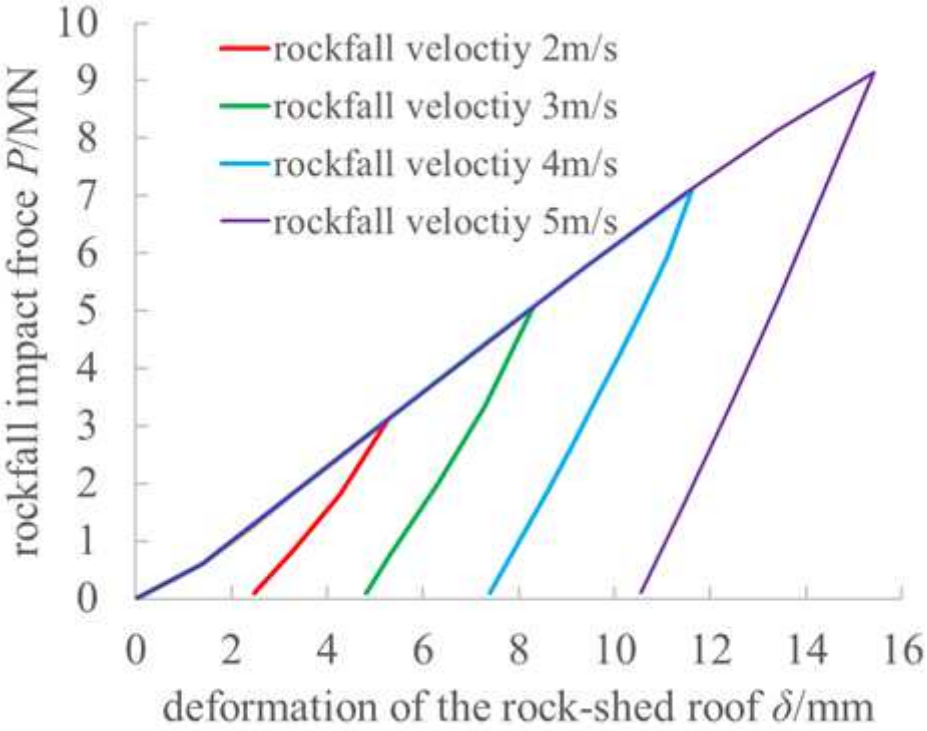

Figure 5

The impact force-deformation curve of the rock-shed roof with different rockfall velocitiy

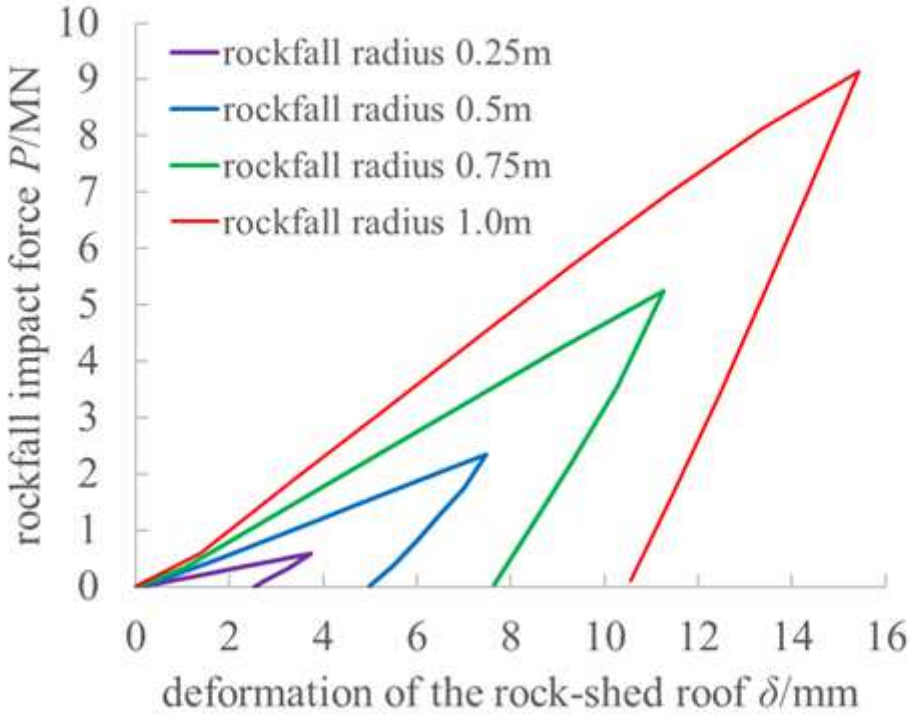

Figure 6

The impact force-deformation curve of the rock-shed roof with different rockfall radius

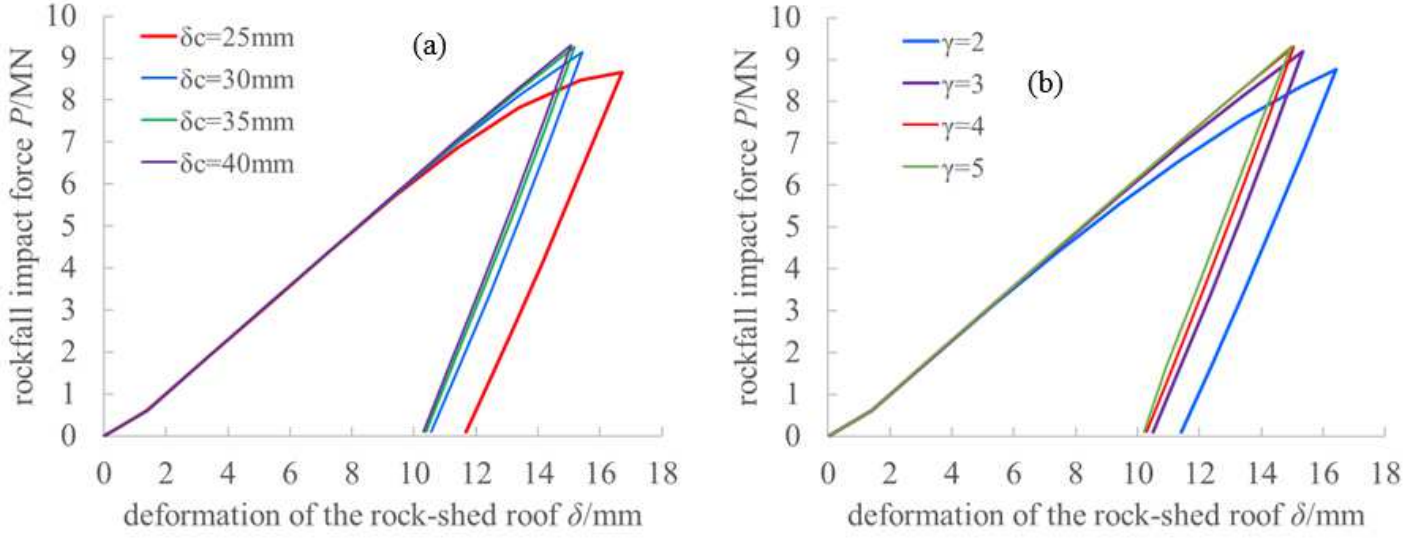

Figure 7

The impact force-deformation curve of the rock-shed roof with different damage parameters

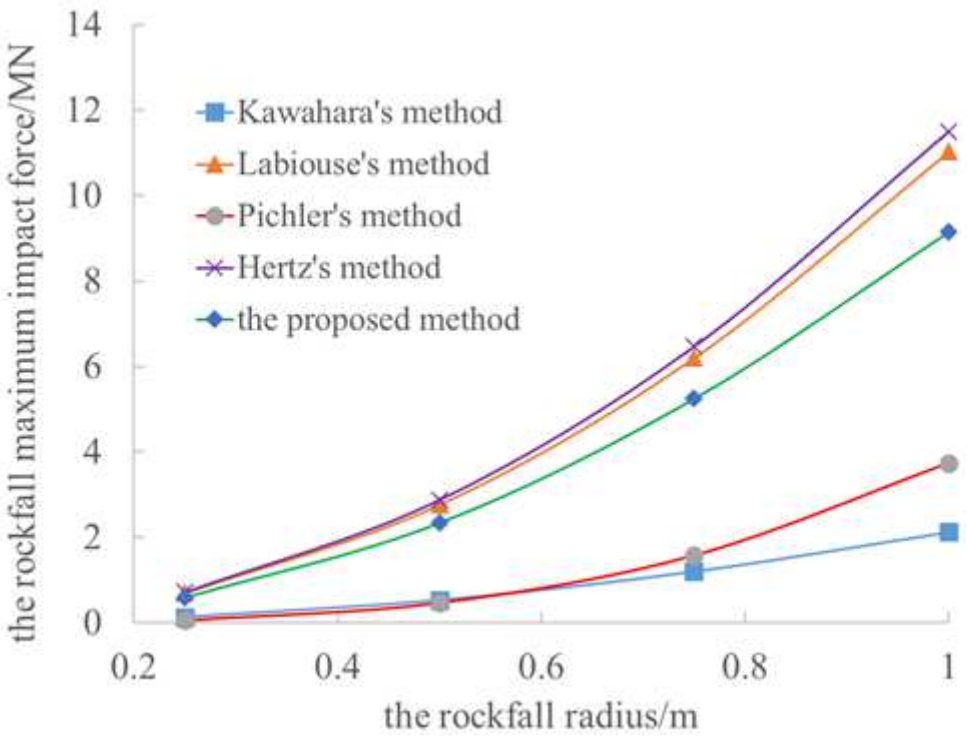

Figure 8

Comparison of the rockfall maximum impact force obtained with the proposed method and other methods